Accepted Manuscript

An intelligent control of NH_3 injection for optimizing the NO_x/NH_3 ratio in SCR system

Guofu Liu, Wenyun Bao, Wei Zhang, Dekui Shen, Qi Wang, Chao Li, Kai Hong Luo

Please cite this article as: G. Liu, W. Bao, W. Zhang, D. Shen, Q. Wang, C. Li, K. Luo, An intelligent control of NH_3 injection for optimizing the NO_x/NH_3 ratio in SCR system, *Journal of the Energy Institute* (2018), doi: https://doi.org/10.1016/j.joei.2018.10.008.

NO$_x$ flux distribution

Weight Analysis

AIG cross section

Non-uniform inlet boundary

guide plate

V. m/s

C. ppm

Sensitivity analysis

NO flux

Condition 1 ... Condition 7

Coordinate Z /m

Coordinate X /m

Valve No.1L
Valve No.13U

weight /non-dimensional

load /MW

Optimized NO$_x$/NH$_3$ mixing ratio   Achieve

Ammonia (NH$_3$)   Nitrogen oxides (NO$_x$)

An intelligent control of NH_3 injection for optimizing the NO_x/NH_3 ratio in SCR system

Guofu Liu[a], Wenyun Bao[b], Wei Zhang[b], Dekui Shen[a, *], Qi Wang[c, d, *], Chao Li[e]

Kai Hong Luo[f]

[a] Key Laboratory of Energy Thermal Conversion and Control of Ministry of Education, Southeast University, Nanjing 210096, Jiangsu, China

[b] Datang Environment Industry Group Co., Ltd, Nanjing 210008, Jiangsu, China

[c] Nanjing Automatic Instrument Automation Co., Ltd, Nanjing 21111, Jiangsu, China

[d] School of measurement and testing engineering, China Jiliang University, Hangzhou 310018, Zhejiang, China

[e] Nanjing Beyond Environmental Engineering Co., Ltd, Nanjing 21111, Jiangsu, China

[f] Department of Mechanical Engineering, University College London, London WC1E 7JE, UK

Abstract: The distribution of nitrogen oxides (NO_x) flux within the cross-section area in front of ammonia injection grid (AIG) under different operating conditions was obtained by computational fluid dynamics (CFD) method. Weight of NO_x flux in the sub-zone corresponding to each of the ammonia (NH_3) injection branch-pipes of AIG system was analyzed and the sensitivity of which against the plant power load was figured out. A number of "critical" ammonia injection branch-pipes were determined with regard to the weight sensitivity analysis. The selected "critical" branch-pipes were changed to be controlled by the automatic valves, and an intelligent tuning strategy was proposed. The NO_x/NH_3 mixing stoichiometry over the cross-section area in front of AIG system was significantly modified for the high utilization ratio of ammonia. A case work was launched on the selective catalytic reduction (SCR) system of a 660 MW plant. As a result, the ammonia consumption rate (ACR) was found to be reduced by 6.44% compared to that under previous control system, and was 9.31% lower than that of the unapplied system. The methodology for determining the "critical" branch-pipes and intelligent tuning strategy of ammonia injection notably saved the ammonia consumption of SCR system, and the formation of ammonium bisulfate (ABS) were greatly confined.

Key Words: SCR system, NO_x flux distribution, ammonia injection grid, intelligent control, ammonium bisulfate

1. Introduction

Nowadays, NO_x serving as a class of nitrogen-containing atmospheric pollutant have been attracting more and more public attention [1,2]. Coal-fired power plants in China which used to be the largest source of NO_x is being compulsively carried out a retrofit of ultra-low emission with respect to NO_x. It is regulated that the

* Corresponding author: Dekui Shen, E-mail: 101011398@seu.edu.cn.
* Corresponding author: Qi Wang, E-mail: wangqi@cjlu.edu.cn.

38 concentration of NO_x emission from coal-fired power plants with the capacity above
39 300MW should be lower than 50mg/m^3 before 2020 [3,4]. Otherwise, those
40 substandard units would be forced to shut down.

41   SCR flue gas denitrification technology has been widely adopted in most
42 coal-fired power plants due to its mature technique and high efficiency. More
43 importantly, the SCR flue gas denitrification technology can be readily controlled in
44 terms of the molar ratio of ammonia to nitrogen, the characteristics of catalyst and so
45 on [5-8]. In a typical ultra-low emission retrofit, three-layer SCR catalyst technique
46 was generally applied. The denitrification efficiency was found to be greatly
47 improved when the reaction time between catalyst and flue gas was being properly
48 prolonged. It needs to be noted that a remarkable increase in the concentration of
49 sulfur trioxide (SO_3) occurred at the exit of SCR system due to the strong oxidation of
50 the commercial catalyst employed [9-11]. On the other hand, the ammonia escape at
51 the exit of SCR system was also found to obviously increase resulting from the
52 inferior operation strategy of NH_3 injection [12]. The gaseous ABS was massively
53 generated due to the simultaneous increase of the ammonia escape, which was prone
54 to be condensed at the cold-side of air preheater. The strong stickiness of ABS (liquid
55 phase) was open to adhere fly ash of the flue gas to the wall of air preheater [13]. As a
56 result, the problems of ash accumulation and corrosion of the cold-side of air
57 preheater were suffered, which consequently led to the increasing flow resistance of
58 flue gas and even the decline of boiler efficiency [14-16].

59   Due to the difficulty in directly controlling the SCR catalyst, to reduce ammonia
60 escape appears to be the key point to ensure the safe and economical operation of the
61 unit after retrofit. Among various techniques adopted, the tuning of NH_3 injection has
62 been considered as the most feasible and promising one [17-19].

63   A great inhomogeneity of the velocity of flue gas and the concentration of NO_x
64 can be observed in the entrance section of SCR system owing to the operation
65 adjustment of the boiler, the transformation of the structural parameters of the flue,
66 and so on [20-23]. The NO_x flux in the sub-zone of the cross-section in front of AIG
67 varied with the power load of plant [24]. Accordingly, it is difficult to make the
68 NO_x/NH_3 mixing ratio in SCR system approximate the desired ratio based on the
69 traditional NH_3 injection strategy (equal or fixed distribution mode). Herein, a
70 strategy for the intelligent automatic tuning of NH_3 injection in SCR system matching
71 the concrete distribution characteristics of NO_x flux is highly required via the
72 optimization of NO_x/NH_3 mixing ratio.

73   A technique for analyzing the weight of NO_x flux in the sub-zone corresponding
74 to each NH_3 injection branch-pipe in AIG system was proposed together with the
75 weight sensitivity of the branch-pipe. The "critical" ammonia injection branch-pipes
76 of AIG system were determined with regard to the weight sensitivity analysis, giving
77 the intelligent ammonia injection strategy. After the launch of the technology on the
78 SCR system of a 660 MW power plant, it was found that the ammonia consumption
79 of SCR system can be notably saved, while the formation of ABS and the corrosion of
80 cold-side of air preheater was confined.

81 2. Research method

82 *2.1. Object of the case work*

83   One side of a SCR system with the capacity of 660 MW was studied in this paper,
84 which had been achieved the requirement of ultra-low emission through the method of
85 three-layer catalyst arrangement. A three-dimensional full scale geometry model with
86 the 40 separate inlet boundaries and 5 internal guide plates was established including
87 the flue between the inlet of the SCR system and the cross-section of AIG, as shown
88 in Fig. 1. The total number of meshes in the case was about 1.01 million.
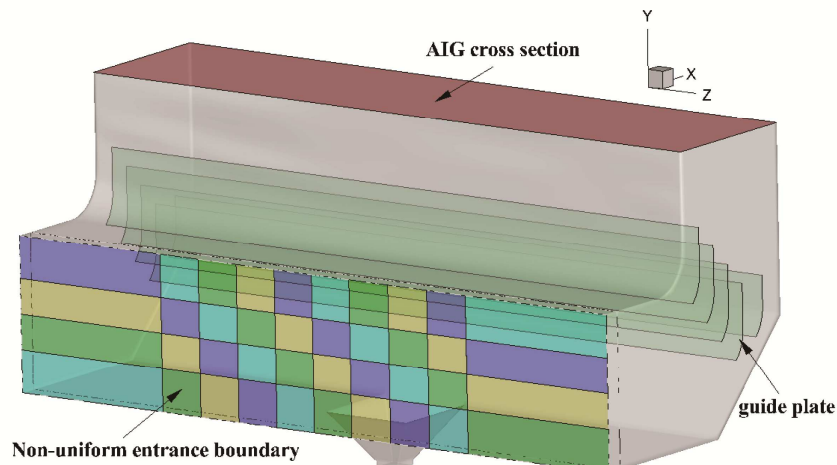
89

90   **Fig. 1.** A geometry model established in the case.

91   A district controlled AIG with different branching inject groups of three types
92 was adopted in the object studied of the case work, which was composed of 14
93 identical branching inject groups for each type. The mixed gas of NH_3 and air is
94 injected to the flue by the above 42 branching inject groups. Accordingly, 42 manual
95 butterfly valves with the function of tuning the amount of gas injected were installed
96 on each main-pipe of 42 branching inject groups. These manual butterfly valves could
97 be divided into three types corresponding to the division criteria of branching inject
98 groups, and they were numbered U, M, L in turn, which is respectively the initials of
99 upper, middle, and lower. The total amount of the mixed gas to participate the
100 denitrification reaction was redistributed through such a district controlled AIG on the
101 basis of the NO_x flux distribution in the flue.

102 *2.2. Acquisition and utilization of non-uniform inlet boundary*

103   The velocity and NO_x concentration of flue gas against 7 sets of stable load
104 conditions were obtained through the 10 temporary test holes available at the entrance
105 position of the SCR system studied. Discrete measurement grid of 40 nodes within the
106 inlet cross-section of the SCR system was set up with the arrangement of total 4
107 measuring depths of 500mm, 1200mm, 1900mm and 2600mm for each temporary test
108 hole. As a result, the corresponding 40 sub-zones controlled by 40 discrete-nodes at
109 the inlet position were formed hypothetically. The NO_x flux distribution on the said 40
110 discrete-nodes in the inlet cross-section of the SCR system was acquired through the

111 product of velocity and NO_x concentration of flue gas on the corresponding
112 discrete-node. The actual amount of NO_x passing through those 40 controlled
113 sub-zones could be accurately described by employing the index of NO_x flux.

114 The final values adopted of the NO_x concentration or velocity on each
115 discrete-node was obtained through the arithmetic mean of 3 sets of the measured
116 records to ensure the accuracy of data acquisition. The measurement of each set of the
117 flue gas velocity was realized by using a micro pressure gauge and a pitot tube of S
118 type with a correction factor of 0.85, and the NO_x volume concentration of each set
119 was carried out through applying the Testo 350 smoke analyzer. The transformation of
120 NO_x mass concentration and the standard state, the introduction of the area of the
121 corresponding controlled sub-zone should be carried out to obtain the final NO_x flux
122 distribution.

123 Thus, a non-uniform inlet boundary closely associated with the operating
124 characteristics of the SCR system studied was formed based on the 40 sub-zones of
125 discrepant input parameters from an overall perspective. But from a local point of
126 view, a uniform inlet boundary within each sub-zone was adopted according to the
127 mean of the data acquisition.

128 In this case, the parameters of the velocity inlet boundary condition and
129 component transport model were closely related to the area of the corresponding
130 sub-zone and the final adopted measured values on each discrete-nodes. The specific
131 inlet boundary parameters of the 600MW load condition could be found in the table
132 S1 of supplementary material, and the component of the flue gas was simplified as a
133 mixture of NO and N_2.

2.3. Analytic method of NO_x flux weight and sensitivity for the sub-zone of each
135 *branch-pipe*

136 The method to determine the weight of NH_3 injection branch-pipe was put
137 forward based on the NO_x flux distribution of the cross-section in front of AIG, which
138 can be described as Eqs. (1). The weight of the branch-pipe i shows the ratio of the
139 NO_x flux in the sub-zone of the AIG cross-section controlled by branch-pipe i to the
140 NO_x flux in the whole AIG cross-section.

$$\varphi_i = f_i / f_{mean} \tag{1}$$

142 where φ_i, f_i, f_{mean} represented the weight of branch-pipe i, the NO_x flux
143 within the sub-zone of the AIG cross-section controlled by branch-pipe i and the mean
144 of NO_x flux in the whole AIG cross-section, respectively.

145 In view of the variation characteristic of the NO_x flux distribution, the weight of
146 each AIG branch-pipe was further investigated under variable power load. The
147 analysis of the weight sensitivity for each AIG branch-pipe was conducted according
148 to the empirical formula in Eqs. (2).

$$max\{|\partial\varphi_i/\partial L|\} \geq \varepsilon \tag{2}$$

150   where L, ε represented the power load and the empirical coefficient of
151   sensitivity judgment of AIG branch-pipe, respectively.

152   The left of the above Eqs. (2) represents the maximum value of the variation
153   slope which could be obtained by analyzing the variation of the branch-pipe weight
154   with the power load. According to the given coefficient of sensitivity judgement ε,
155   the AIG branch-pipe i would be considered critical and sensitive if the empirical Eqs.
156   (2) is established.

157   The corresponding relationship between the weight and the opening of AIG
158   branch-pipe valves could be described as Eqs. (3). The opening of the 42 AIG
159   branch-pipe valves must be kept within the range of 0~1, in case of a frequent or
160   sharp change in the opening of any valves to ensure a stable operation of the SCR
161   system. The compression coefficient CP must be introduced to meet the above
162   requirements (Eqs. (3)).

163
$$ON_i = \overline{ON} + \frac{\varphi_i}{CP} \geq \varepsilon \qquad (3)$$

164   where ON_i, $\overline{ON}$, CP represented the opening of AIG branch-pipe valve i, the
165   base average opening of the 42 AIG branch-pipe valves and the compression
166   coefficient, respectively.

167   The compression coefficient CP introduced here was an empirical coefficient
168   related to the maximum weight and the average opening of the 42 AIG branch-pipe
169   valves, and its empirical formula can be shown in Eqs. (4). All the 42 AIG
170   branch-pipe valves could work reasonably in all conditions through a reasonable
171   compression coefficient adopted.

172
$$CP \geq \frac{max\{\varphi_i\}}{1-\overline{ON}} \qquad (4)$$

173   where $max\{\varphi_i\}$ represented the maximum weight of the 42 AIG branch-pipe
174   valves in all studied conditions.

175   3. Results and discussion

176   *3.1. The distribution of NO$_x$ flux over the cross-section area in front of AIG*

177   According to the non-uniform inlet boundary acquired at the entrance position of
178   the SCR system, the NO$_x$ flux distribution within the cross-section in front of AIG
179   was obtained indirectly under 7 sets of stable load conditions including 300, 350, 400,
180   450, 500, 550 and 600MW as shown in Fig. 2(a)~(g). Relevant studies shown that the
181   concentration of NO$_x$ produced by the combustion of pulverized coal was greatly
182   affected by many factors, such as coal species, combustion mode and so on [25-28].

183   As can be seen from Fig. 2(a)~(g), the mean of the NO$_x$ flux within the
184   cross-section in front of AIG shows a rough trend of continuous growth with the
185   increase of the power load. It is worth mentioning that the amount of flue gas
186   generated grows accordingly with the increase of the power load. It hence can be
187   inferred that the velocity of flue gas should also be considered as an important index

188   in characterizing the actual amount of NO$_x$ passing, which could be employed to
189   evaluate the actual amount of NO$_x$ passing.
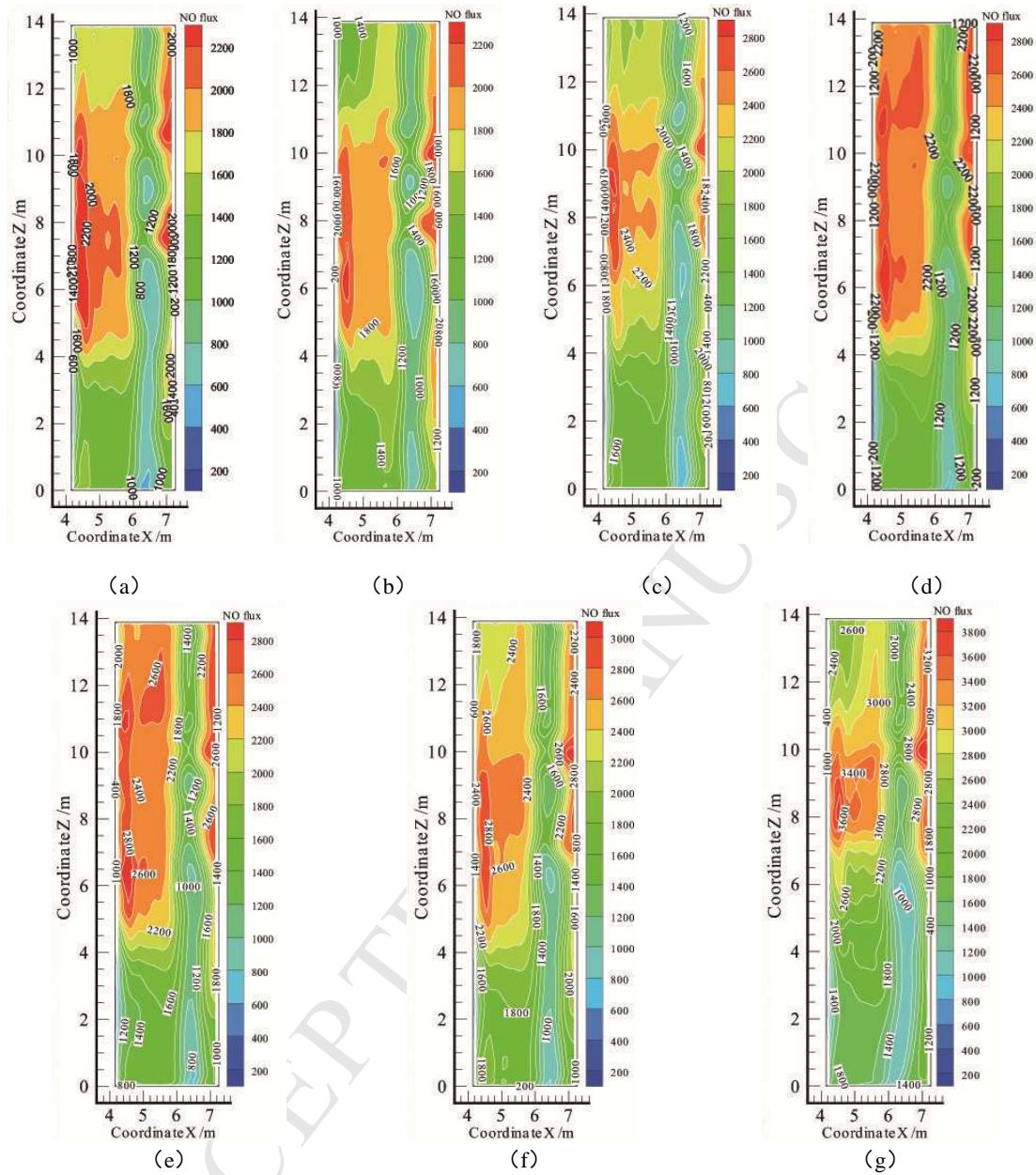
190   **Fig. 2.** The NO$_x$ flux distribution within the cross-section in front of AIG under the load condition
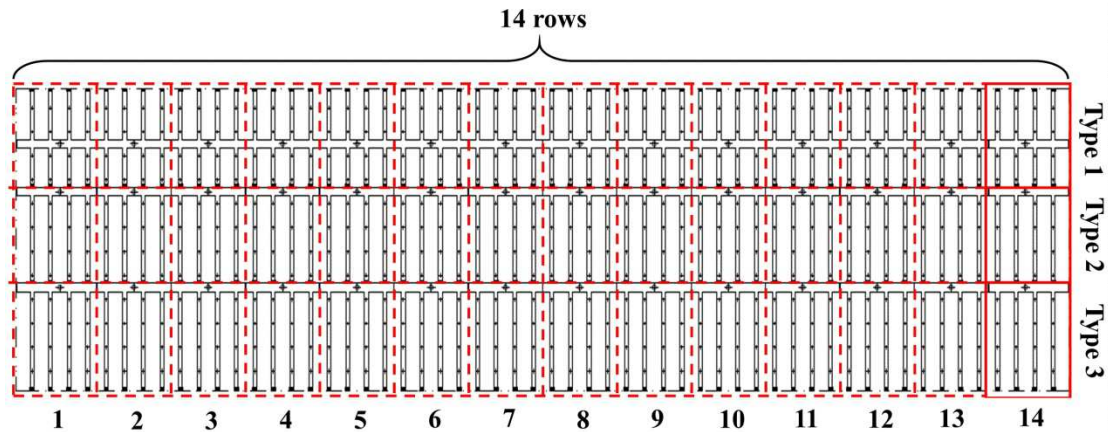191   of 300(a), 350(b), 400(c), 450(d), 500(e), 550(f), 600MW(g).

14 rows

Fig. 3. The corresponding structure of AIG.

As shown in Fig. 3, the NO_x flux distribution within the cross-section in front of AIG was further analyzed in terms of the corresponding structure of AIG. It was found that the NO_x flux distribution under individual power load condition exhibited a pronounced non-uniformity. The average deviation of NO_x flux distribution was 28.94%. Particularly, the maximum deviation of NO_x flux distribution was derived from 600MW load condition which was up to 32.87%. Accordingly, the NO_x/NH_3 mixing ratio within the cross-section of AIG relying on the uniform injection should be improved.

The non-uniform characteristic of the NO_x flux distribution varied with the power load condition, especially for each sub-zone within the AIG cross-section. The cross-section in front of AIG could also be divided into 42 hypothetical sub-zones which correspond to the 42 AIG branch-pipes. And the variation characteristic of the NO_x flux within each sub-zone is completely different. For example, it can be seen that the NO_x flux in one sub-zone exhibited obvious variation with the power load while the NO_x flux in another sub-zone maintained at a relatively stable level regardless of the change of load conditions. Thus, the tuning strategy of NH_3 injection should be analyzed concretely for different branch-pipes according to the variation characteristic of the NO_x flux within corresponding sub-zone.

3.2. Analysis of NOx flux weight and sensitivity of each branch-pipe

The distribution of NO_x flux over the cross-section area in front of AIG was evaluated quantitatively by analyzing the weight of the branch-pipe based on the Eq (1). It was found that the weights of the 42 AIG branch-pipes showed different variation characteristics. Several typical variation characteristics of these branch-pipes are shown in Fig. 4 with the function of the power load ranging from 300 to 600MW.

As can be seen from Fig. 4(a), the variation characteristic of the weight of branch-pipe 1L and 13U was similar to the cubic curve with relatively severe variation, and their corresponding maximum deviation of the weight is 33.95% and 39.13% respectively. It can be inferred that the NO_x flux distribution in the sub-zone in front of AIG controlled by branch-pipe 1L or 13U is strongly affected by the variation of the power load condition. Similarly, as can be seen from Fig. 4(b), the variation characteristic of the weight of branch-pipe 5U and 13L was close to a quadric curve either with a downward or upward opening. The maximum deviation of

226 the weight calculated of 5U and 13L is as high as 51.49% and 33.86%, respectively.
227 This indicated that the NO_x flux distribution in the sub-zone in front of AIG controlled
228 by these two branch-pipes was strongly affected by the variation of the power load
229 condition. However, the variation characteristic of the weight of branch-pipe 8M and
230 7M showed a different trend compared with the above two cases which can be seen
231 from Fig. 4(c). It can be seen that the weight variation curve of branch-pipe 8M or 7M
232 is approximately consistent with the horizontal line, and the maximum deviation of
233 the weight calculated is only 14.58% for 8M and 9.80% for 7M. It can be concluded
234 that the NO_x flux distribution in the sub-zone in front of AIG controlled by
235 branch-pipe 8M and 7M was basically stable instead of being easily affected by other
236 factors. The variation characteristic of the weight of the other 36 branch-pipes could
237 be summed up into the above three types.
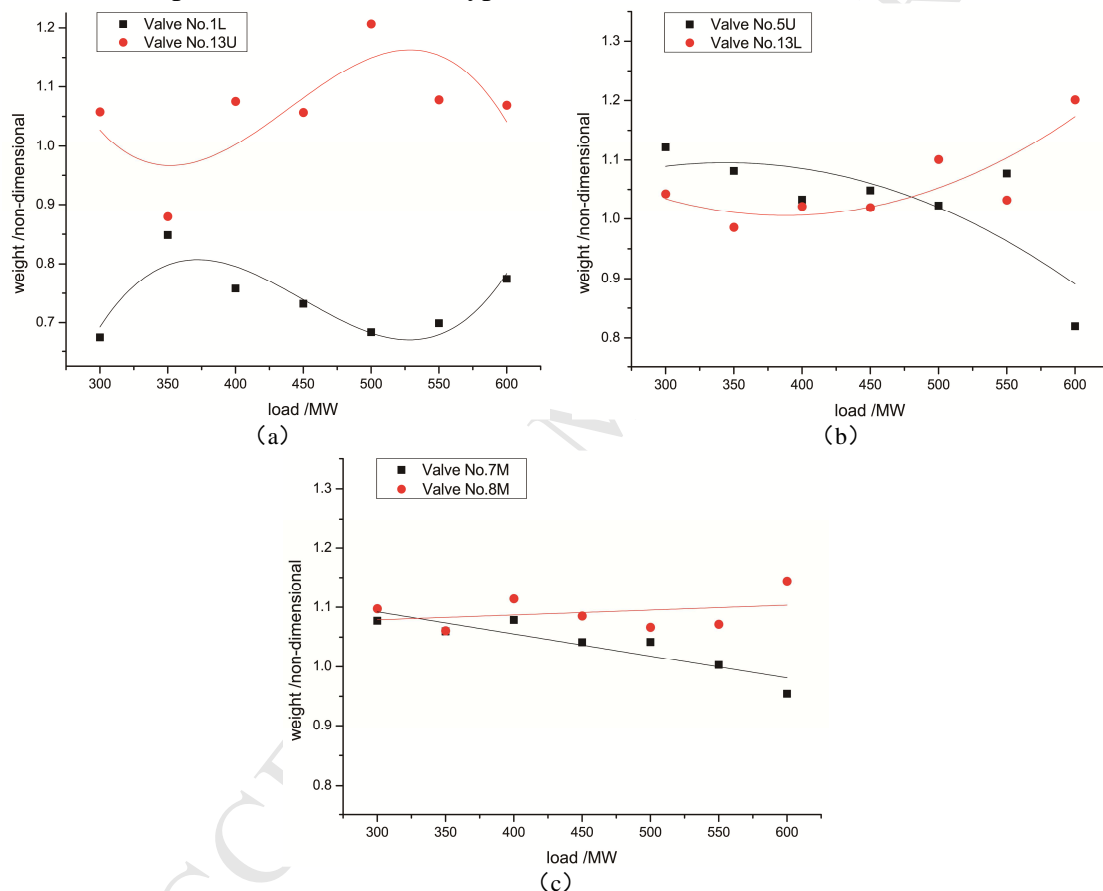
Fig. 4. Variation characteristics of the weight of several typical branch-pipes.

239 The tuning strategy of NH_3 injection for branch-pipe i should be matched with
240 the variation characteristic of the weight of branch-pipe i combined with the
241 mechanism of SCR denitrification. In other words, where the amount of the NO_x
242 passing through changes, the amount of NH_3 injection should be tuned accordingly.
243 Thus, the manual valves installed on the branch-pipes with stronger variation
244 characteristic of the weight should be converted into automatic regulating valves to
245 realize the automatic tuning of NH_3 injection against the power load, such as
246 branch-pipe 1L, 13U, 5U and 13L. On the other hand, the opening of the manual
247 valves that installed on the branch-pipes with mild variation characteristic of the
248 weight should be tuned to a fixed value that optimized through all load conditions

249 studied, such as branch-pipe 8M and 7M. Based on the principle of weight sensitivity
250 judgment showed in Eqs. (2), the manual "critical" valves that needed to be automatic
251 retrofit could be determined through analyzing the variation of the branch-pipe weight
252 with the power load. A total of 11 "critical" NH_3 injection branch-pipes of AIG system
253 is determined in this case work including 5U, 6U, 14U, 13U, 9U, 12U, 1M, 10U, 1L,
254 1U and 13L. The empirical coefficient of sensitivity judgment adopted here was
255 0.33%.

3.3. The intelligent ammonia injection strategy

257 The automatic tuning strategy of NH_3 injection for each branch-pipe could be
258 obtained based on the corresponding relationship between the weight and the opening
259 of AIG branch-pipe valves shown in the Eqs. (3). However, the operational reliability
260 of the automatic regulating valves reformed must avoid any frequent or sharp change
261 in the opening of valves. Accordingly, the empirical compression coefficient *CP* as
262 shown in Eqs. (4) is introduced to ensure the stable and safe operation of all 42 AIG
263 branch-pipe valves. An intelligent ammonia injection strategy for the "critical"
264 branch-pipes could be developed for engineering application after the retrofit of
265 automatic control valves for "critical" valves.
266 The variation of NO_x flux in the sub-zone controlled by the corresponding
267 "critical" branch-pipes is consistent with the weight variation law. The weight of
268 "critical" branch-pipes related to the NO_x flux in the sub-zone is significantly changed
269 when the plant load is varied (Fig. 4). The opening of the "critical" branch-pipes
270 valves would be changed accordingly with the help of the intelligent ammonia
271 injection strategy, The NO_x/NH_3 ratio in the area can be greatly improved, leading to
272 higher denitrification efficiency and less ammonia escape.
273 In this case work, the base average opening of the 42 AIG branch-pipe valves
274 was set to 0.5 empirically, and the minimum compression coefficient CP_{min} was
275 calculated to be 2.9686 accordingly. The compression coefficient *CP* adopted finally
276 should be larger than CP_{min} in order to keep the opening of the branch-pipe valves
277 within the range of 0~1. And the pressure loss of AIG system would be too high when
278 the *CP* taken is too large, which is not conducive to the safe and economic operation
279 of SCR system. So the empirical compression coefficient *CP* taken finally was set to
280 3.325 with comprehensive consideration of above influences. As a result of that, the
281 actual average opening of the 42 AIG branch-pipe valves is about 0.8, with the
282 maximum of 0.95 and the minimum of 0.69.
283 Finally, an intelligent ammonia injection strategy of automatic regulating against
284 power load was proposed for the 11 "critical" branch-pipe valves, while the opening
285 of the "uncritical" branch-pipe valves was tuned to a fixed value that optimized
286 through all load conditions studied. It is worth noting that the ammonia injection
287 strategy of "critical" or "uncritical" branch-pipe valves was both obtained base on the
288 analysis of NO_x flux distribution within the cross-section in front of AIG.

3.4. Analysis of the application case

290 The optimized ammonia injection strategy has been applied on the A side of the
291 SCR system while the B side was not applied serving as the contrast one. The ACR

292 was adopted to evaluate the application effect of the optimized ammonia injection
293 strategy as shown in Eqs. (5). The rate of the ammonia consumed to the NO_x removed
294 could be quantitative described through the dimensionless index of ACR. And it can
295 be inferred that the lower the value of ACR, the higher the utilization rate of ammonia
296 obviously.

297
$$ACR = M_a / \left[\left(C_{nox}^{in} - C_{nox}^{out} \right) Q_f \right] \quad (5)$$

298 where M_a(mg·h^{-1}), C_{nox}^{in}(mg·Nm^{-3}), C_{nox}^{out}(mg·Nm^{-3}), Q_f(Nm^3·h^{-1}) represented

299 the mass flow of ammonia consumed, the mass concentration of inlet NO_x, the mass
300 concentration of outlet NO_x and the volume flow of flue gas, respectively.
301 The application effect of the optimized ammonia injection strategy can be
302 analyzed from both lateral and vertical aspects. The operating data of 5 whole days of
303 A and B side were used to analyze the average ACR of the SCR system before and
304 after the application of the intelligent optimized ammonia injection strategy, which
305 were shown in Fig. 5.
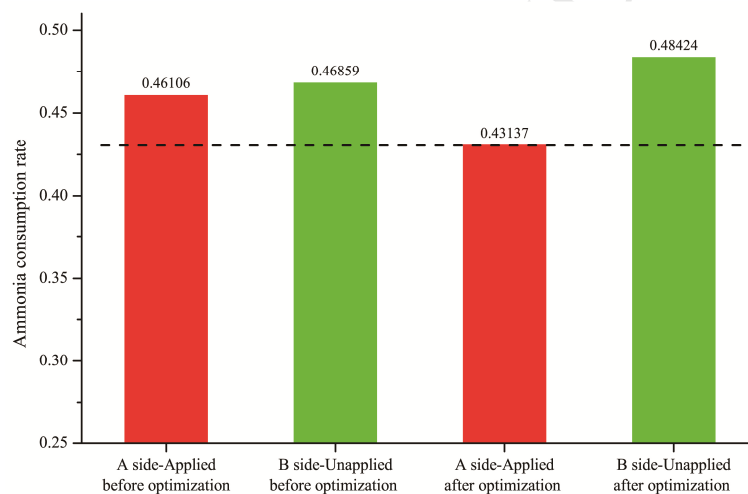
307 **Fig. 5.** The average ACR before and after optimization in the case work.

308 As can be seen from the Fig. 5, the average ACR values of A and B sides were
309 comparable before the application of optimized intelligent ammonia injection strategy.
310 The difference of the average ACR values between the two sides was only 1.61%.
311 However, that difference was increased to about 10.92% after the optimization in A
312 side. Accordingly, it can be calculated that the ACR of A side optimized was about
313 9.31% lower than that of B side. In addition, the average ACR of A side reduced from
314 0.46106 to 0.43137 with a decrease of about 6.44%. Therefore, it can be concluded
315 that the average ACR of the SCR system would be remarkably reduced as the
316 application of the optimized intelligent ammonia injection strategy, which would
317 optimize the NO_x/NH_3 mixing ratio, reduce the ammonia escape, confine the
318 formation of ABS and the corrosion of cold-side of air preheater.

319 4. Conclusions

320 Weight of NO_x flux of the sub-zone corresponding to each ammonia injection

321 branch-pipe in AIG system was analyzed, sensitivity of which was correlated to the
322 structure of AIG under different operating conditions. The determination of "critical"
323 injection branch-pipes and the intelligent tuning strategy was proposed. It was found
324 that the ammonia consumption of SCR system was notably saved with the change of
325 the "critical" branch-pipe valve and application of the intelligent tuning strategy.

329 References

330 [1] T. Boningari, P.G. Smirniotis, Impact of nitrogen oxides on the environment and
331   human health: Mn-based materials for the NOx abatement, Current Opinion in
332   Chemical Engineering 13 (2016) 133-141.
333 [2] P. Glarborg, A.D. Jensen, J.E. Johnsson, Fuel nitrogen conversion in solid fuel
334   fired systems, Progress in Energy and Combustion Science 29(2) (2003) 89-113.
335 [3] W.Z. Shi, M.M. Yang, X.H. Zhang, S.Q. Li, Q. Yao, Ultra-low emission technical
336   route of coal-fired power plants and the cooperative removal, Zhongguo Dianji
337   Gongcheng Xuebao/Proceedings of the Chinese Society of Electrical Engineering
338   36(16) (2016) 4308-4318.
339 [4] Q.Y. Li, W. Meng, G.C. Wu, J. Zhang, S.Q. Zhu, D.Q. Hu, C.H. Zheng, X. Gao,
340   R.N. Wang, H.J. Liu, Evaluation on operation state and stability for denitrification
341   of ultra low emission, Zhejiang Daxue Xuebao (Gongxue Ban)/Journal of
342   Zhejiang University (Engineering Science) 50(12) (2016) 2303-2311.
343 [5] L. Deng, X. Liu, P. Cao, Y. Zhao, Y. Du, C.A. Wang, D. Che, A study on
344   deactivation of V2O5-WO3-TiO2 SCR catalyst by alkali metals during
345   entrained-flow combustion, Journal of the Energy Institute 90(5) (2016) 743-751.
346 [6] F.Y. Gao, X.L. Tang, H.H. Yi, S.Z. Zhao, C.L. Li, J. Li, Y. Shi, X. Meng, A Review
347   on Selective Catalytic Reduction of NOx by NH3 over Mn–Based Catalysts at
348   Low Temperatures: Catalysts, Mechanisms, Kinetics and DFT Calculations,
349   Catalysts 7(7) (2017) 1-32.
350 [7] Y.J. Yang, J. Liu, Z. Wang, F. Liu, A skeletal reaction scheme for selective
351   catalytic reduction of NO x with NH 3 over CeO 2 /TiO 2 catalyst, Fuel
352   Processing Technology 174 (2018) 17-25.
353 [8] J. Xiang, P.Y. Wang, S. Su, L. Zhang, F. Cao, Z. Sun, X. Xiao, L. Sun, S. Hu,
354   Control of NO and Hg0 emissions by SCR catalysts from coal-fired boiler, Fuel
355   Processing Technology 135 (2015) 168-173.
356 [9] J.X. Wang, J.F. Miao, W.J. Yu, Y.T. Chen, J. Chen, Study on the local difference of
357   monolithic honeycomb V2O5-WO3/TiO2 denitration catalyst, Materials
358   Chemistry and Physics 198 (2017) 193-199.
359 [10] X.Q. Wang, A.J. Shi, Y.F. Duan, J. Wang, M.Q. Shen, Catalytic performance and
360   hydrothermal durability of CeO2–V2O5–ZrO2/WO3–TiO2 based NH3-SCR
361   catalysts, Catalysis Science & Technology 2(7) (2012) 1386-1395.

[11] X.P. Zhang, B.X. Shen, J.H. Chen, J. Cai, C. He, K. Wang, Mn-0.4/Co0.1Ce0.45Zr0.45Ox, high performance catalyst for selective catalytic reduction of NO by ammonia, Journal of the Energy Institute 86(2) (2013) 119-124.

[12] Y. Gao, T. Luan, T. LÜ, K. Cheng, H.M. Xu, Performance of V2O5-WO3-MoO3/TiO2 Catalyst for Selective Catalytic Reduction of NOx by NH3, Chinese Journal of Chemical Engineering 21(1) (2013) 1-7.

[13] Y.F. Bu, L.M. Wang, X. Chen, X.Y. Wei, L. Deng, D. Che, Numerical analysis of ABS deposition and corrosion on a rotary air preheater, Applied Thermal Engineering 131 (2018) 669-677.

[14] L. Muzio, S. Bogseth, R. Himes, Y.-C. Chien, D. Dunn-Rankin, Ammonium bisulfate formation and reduced load SCR operation, Fuel 206 (2017) 180-189.

[15] Y.J. Shi, H. Shu, Y.H. Zhang, H.M. Fan, Y.P. Zhang, L.J. Yang, Formation and decomposition of NH4HSO4 during selective catalytic reduction of NO with NH3 over V2O5-WO3/TiO2 catalysts, Fuel Processing Technology 150 (2016) 141-147.

[16] Y.Z. Fan, F.H. Cao, Thermal Decomposition Kinetics of Ammonium Sulfate, Journal of Chemical Engineering of Chinese Universities 25(2) (2011) 341-346.

[17] S. Shah, S. Abrol, S. Balram, et al, Optimal Ammonia Injection for Emissions Control in Power Plants, IFAC-PapersOnLine 48(30) (2015) 379-384.

[18] Y.B. Wang, H.Z. Tan, K. Dong, H.X. Liu, J.F. Xiao, J. Zhang, Study of ash fouling on the blade of induced fan in a 330 MW coal-fired power plant with ultra-low pollutant emission, Applied Thermal Engineering 118 (2017) 283-291.

[19] K.K. Zhang, J. Zhao, Y.C. Zhu, MPC case study on a selective catalytic reduction in a power plant, Journal of Process Control 62 (2018) 1-10.

[20] N. Usberti, M. Jablonska, M.D. Blasi, P. Forzatti, L. Lietti, A. Beretta, Design of a "high-efficiency" NH 3 -SCR reactor for stationary applications. A kinetic study of NH 3 oxidation and NH 3 -SCR over V-based catalysts, Applied Catalysis B: Environmental 179 (2015) 185-195.

[21] Y.H. Gao, Q.C. Liu, L.T. Bian, Numerical Simulation and Optimization of Flow Field in the SCR Denitrification System on a 600 MW Capacity Units, Energy Procedia 14 (2012) 370-375.

[22] Z. Lei, C. Wen, B. Chen, Optimization of internals for Selective Catalytic Reduction (SCR) for NO removal, Environ Sci Technol 45(8) (2011) 3437-3444.

[23] Y.Y. Xu, Y. Zhang, J. Wang, J. Yuan, Application of CFD in the optimal design of a SCR-DeNOx system for a 300MW coal-fired power plant, Computers and Chemical Engineering 49 (2013) 50-60.

[24] G.F. Liu, D.K. Shen, R. Xiao, Optimization and experimental verification of AIG tuning for SCR system of coal-fired power station based on diagnose of flow field, Dongnan Daxue Xuebao (Ziran Kexue Ban)/Journal of Southeast University (Natural Science Edition) 47(1) (2017) 98-106.

[25] M.F. Fu, C.T. Li, P. Lu, L. Qu, M.Y. Zhang, Y. Zhou, M. Yu, Y. Fang, A review on selective catalytic reduction of NOxby supported catalysts at 100–300 °C—catalysts, mechanism, kinetics, Catal Sci Technol 4(1) (2014)

406   14-25.

407 [26] M.H. Song, L.Y. Zeng, X.G. Li, Y.B. Liu, Z.C. Chen, Z.Q. Li, Effects of tertiary
408   air damper opening on flow, combustion and hopper near-wall temperature of a
409   600 MWe down-fired boiler with improved multiple-injection multiple-staging
410   technology, Journal of the Energy Institute 91(4) (2017) 573-583.

411 [27] Y.Q. Niu, T. Shang, J. Zeng, S. Wang, Y. Gong, S.e. Hui, Effect of Pulverized
412   Coal Preheating on NOx Reduction during Combustion, Energy & Fuels 31(4)
413   (2017) 4436-4444.

414 [28] M.Y. Hwang, S.G. Ahn, H.C. Jang, G.B. Kim, C.H. Jeon, Numerical study of an
415   870MW wall-fired boiler using De-NOx burners and an air staging system for low
416   rank coal, Journal of Mechanical Science and Technology 30(12) (2016)
417   5715-5725.

418 Nomenclature

419 SCR: selective catalytic reduction

420 NO_x: nitrogen oxides

421 NH_3: ammonia

422 AIG: ammonia injection grid

423 CFD: computational fluid dynamics

424 ACR: ammonia consumption rate

425 ABS: ammonium bisulfate

426 MW: megawatt

427 SO_3: sulfur trioxide

Journal of the Energy Institute

Highlights

- Weight of NO_x flux in sub-zone of section-cross area in front of AIG was analyzed.

- The "critical" NH_3 injection branch-pipes were determined for intelligent control.

- NO_x/NH_3 ratio in SCR system can be optimized via application of this technology.